# Design and simulation of ZnO-based light-emitting diode structures

Sang Youn Han, Hyucksoo Yang, D. P. Norton, and S. J. Pearton[a)]
*Department of Materials Science and Engineering, University of Florida, Gainesville, Florida 32611*

F. Ren
*Department of Chemical Engineering, University of Florida, Gainesville, Florida 32611*

A. Osinsky, J. W. Dong, B. Hertog, and P. P. Chow
*SVT Associates, Inc., Eden Prairie, Minnesota 55344*

(Received 8 September 2005; accepted 10 October 2005)

Two different types of ZnO-based light-emitting diode structures have been examined using a one-dimensional (1D) simulator that accounts for specific features of the hexagonal semiconductors—strong piezoeffects, existence of spontaneous electric polarization, low efficiency of acceptor activation, and high threading dislocation density (normally, $\sim 10^7 - 10^9$ cm$^{-2}$) in the material. A hybrid ZnO/CdZnO/AlGaN/GaN structure grown on sapphire avoids problems in achieving robust *p*-type doping in ZnO. An all-ZnO approach employs a MgZnO/CdZnO/MgZnO double heterostructure grown on a ZnO substrate. Both structures show a strong sensitivity of emission intensity to doping and layer thicknesses within our simulations. © *2005 American Vacuum Society.* [DOI: 10.1116/1.2131869]

## I. INTRODUCTION

ZnO-based UV light-emitting diode (LED) structures are attracting much interest because of ZnO's high exciton binding energy compared to GaN, the availability of high quality ZnO substrates (enabling the fabrication of vertical geometry devices with low threading dislocation densities) and the simpler processing relative to GaN for which convenient wet etches are not available.[1–3] A number of recent papers have reported ZnO-based light emitting structures, including homojunctions with low emission intensity,[4–6] hybrid structures involving heterostructures with SiC, GaN/sapphire, AlGaN/sapphire or $Cu_2O$,[7–12] and ZnO pin homojunction diodes grown on $ScMgAlO_4$ substrates.[13,14] In the latter case, device performance was limited due to the high spreading resistance of the bottom ZnO layer, suggesting the need for a conducting ZnO substrate. For all these ZnO LED structures, however, the growth has not yet been optimized.

Another important factor in the design of ZnO-based LED is the realization of bandgap engineering to create barrier layers and quantum wells in heterostructures. With respect to higher bandgaps, an increase up to 4.0 eV has been achieved by the incorporation of Mg in the ZnO layer while still maintaining the wurtzite structure.[15] Ternary ZnCdO seems to be an appropriate candidate for narrow bandgap because of the smaller bandgap of CdO. (2.3 eV).[16] In addition, when grown on *c*-plane sapphire, analogous to III-nitride, the total polarization of ZnO is aligned along the [0001] growth direction. Thus, the polarization-induced fields may influence the electronic band structure and carrier concentration profiles of ZnO-base LEDs. Although many factors need to be considered in designing ZnO-based LED, no comprehensive investigation on optimized device structures and their expected performance is currently available. Therefore, there is a clear need for providing some design parameters for the LED structures in terms of layer structure, doping and composition and how they effect light emission intensity and current-voltage ($I$–$V$) characteristics.

In this paper, we describe some simulation results for both the hybrid ZnO/ZnCdO/ZnO/AlGaN/GaN/sapphire substrate structures and the ZnMgO/ZnCdO/ZnO/ZnMgO substrate LEDs. These results will be used to identify the most important parameters for achieving high brightness and high performance.

## II. EXPERIMENTAL

The simulation program used in this study was SILENSE™ code.[17] This is a 1D simulator which can build a band diagram, carrier injection and recombination, and light emission profiles in wide bandgap LED heterostructures. The SILENSE 2.1 version is capable of simulating heterostructures made not only of group-III nitrides, but also of other wurtzite semiconductors (for example, ZnMgO alloys) including hybrid structures. The LED operation of the heterostructure is considered within the framework of the 1D drift diffusion model of carrier transport that accounts for specific features of the nitride semiconductors—strong piezoeffect, existence of spontaneous electric polarization, low efficiency of acceptor activation, and high threading dislocation density (normally, $\sim 10^7 - 10^9$ cm$^{-2}$). Along with bimolecular radiative electron and hole recombination, an original model of nonradiative carrier recombination at threading dislocation cores is also considered. The latter allows an analysis of the interaction between the radiative and nonradiative recombination channels and predicts the internal emission efficiency of the LED structure as a function of threading dislocation density. The spectrum of light emission from a single- or multiple-

a)Electronic mail: spear@mse.ufl.edu

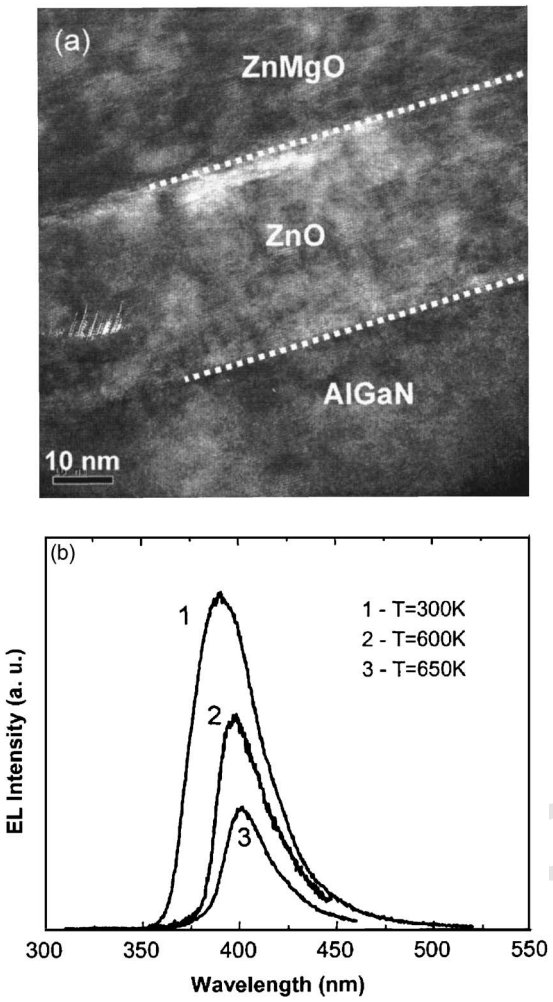


FIG. 1. (a) Cross-sectional TEM image and (b) temperature dependent EL spectrum in ZnMgO/ZnO/AlGaN/GaN LED.

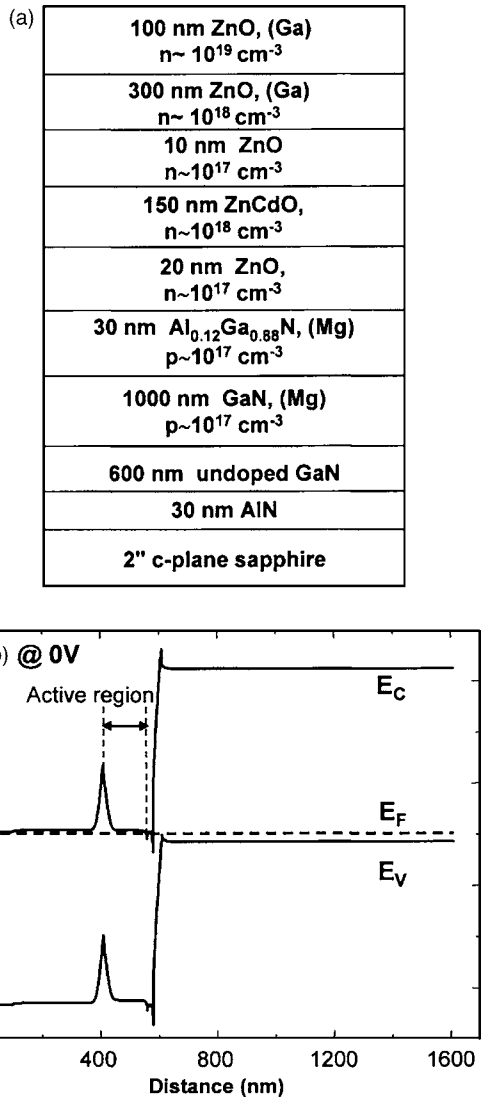


FIG. 2. (a) Schematic of ZnO/ZnCdO/ZnO/AlGaN/GaN structure simulated and (b) its band diagram.

quantum-well active region can be calculated to account for the complex valence band structure of wurtzite semiconductors by using the $8\times8$ Kane Hamiltonian. Energies and wave functions of localized carrier states are found by a numerical solution of the Schrödinger equation within the effective-mass approximation. Generation of the grid for each QW is totally automated.

The model implemented into the code incorporates the following: (i) Localized and distributed polarization charges in the LED structure induced by both spontaneous and piezopolarization in nitride semiconductors; (ii) Fermi statistics for electrons and holes for both degenerate and nondegenerate semiconductors; (iii) partial ionization of donors and acceptors depends on the respective quasi-Fermi level positions; (iv) strain calculations in the LED structure assume coherent growth of all epilayers on an underlying buffer layer; (v) bimolecular radiative electron and hole recombination neglects quantum-confined effects on the recombination rate; and (vi) nonradiative carrier recombination in the principal channel and on threading dislocation cores. The LED $I-V$ characteristics are calculated by the software at a given serial resistance that is assumed to account for both the lateral current spreading in the LED chip and Ohmic contact resistances. Moreover, the light emission spectra are determined with a post-processing module that uses the calculated band profiles of the LED structure and takes into account the complex structure of the valence band of nitride materials and the contribution of the confined electronic states.

In our simulations we used the available ZnMgCdO material parameters,[19–21] but not all the required parameters are available. For example, the band-offsets between ZnMgO/ZnO and ZnCdO/ZnO are not known. Whenever the required parameter was unavailable we used preliminary values obtained from x-ray photoelectron spectroscopy for samples grown by MBE on *c*-plane sapphire. Given the preliminary nature of the available data, the simulated results should be used as a guide for identifying important parameters in the LED design rather than as definitive.

TABLE I. Simulated parameters conducted in ZnO/ZnCdO/ZnO/AlGaN/GaN structure. Bolded conditions in the table correspond to the referenced ones in Fig. 2.

| Parameters | Conditions |
|---|---|
| Active layer thickness | 50, 100, **150**, 200 (nm) |
| Active layer doping | $10^{16}, 10^{17}, \mathbf{10^{18}}, 10^{19}$ ($cm^{-3}$) |
| Active layer composition | Cd composition: 0.03, **0.05**, 0.07 |
| Top cladding layer composition and thickness | **10**, 20, 30 (nm), Mg: 0.1, 0.2 |
| Bottom cladding layer composition and thickness | **20**, 30, 40 (nm), Mg: 0.1, 0.2 |

## III. RESULTS AND DISCUSSION

### A. Hybrid ZnO/GaN LEDs

In our previous work, we observed that hybrid ZnMgO/ZnO/AlGaN/GaN LEDs grown on sapphire substrates showed clean interfaces between the various layers as shown in the transmission electron microscopy images of Fig. 1(a). Moreover, the fabricated LED with this structure operated above 650 K, as observed in temperature dependent electroluminescence spectrum [Fig. 1(b)].[10,11,22] The band structures of various MgZnO/AlGaN/GaN heterojunctions were also simulated, revealing strong hole confinement near the *n*-ZnO/*p*-AlGaN interface with a hole sheet density up to $1.8\times10^{13}$ $cm^{-2}$. The formation of a hole accumulation layer and a triangular well near the hybrid heterointerface can increase the probability of radiative recombination under forward bias.[22] To achieve a broader range of emission wavelengths, ZnCdO active regions have been considered essential due to the controllability of bandgap. Thus, we designed *n*-ZnO/*p*-AlGaN structure with ZnCdO active region.

The schematic cross-sectional diagram of hybrid ZnO/GaN structure and its band diagram are displayed in Fig. 2. The range of the various parameters used in this simulation study is summarized in Table I. The active region is sandwiched by triangular wells arising from the polarization contribution at the interfaces. This implies that the carriers are effectively confined in the active region which can increase the probability of radiative recombination under forward bias. Introduction of the ZnMgO/ZnO heterojunction provides an additional confinement for electrons injected into the ZnCdO active region.

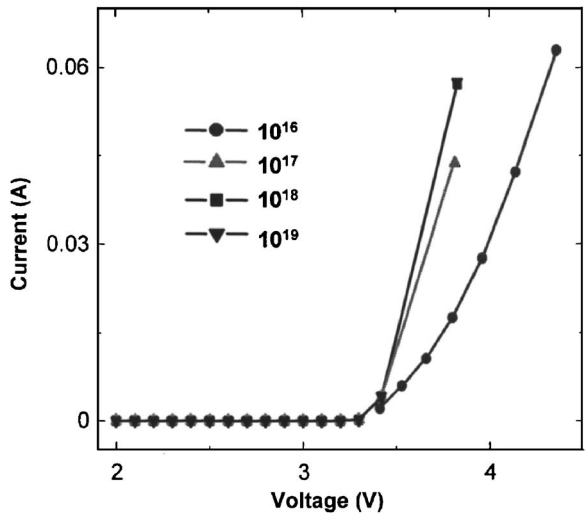


FIG. 3. Simulated *I–V* characteristics of ZnO/ZnCdO/ZnO/AlGaN/GaN structure as a function of active layer doping at fixed Cd composition of 0.05.

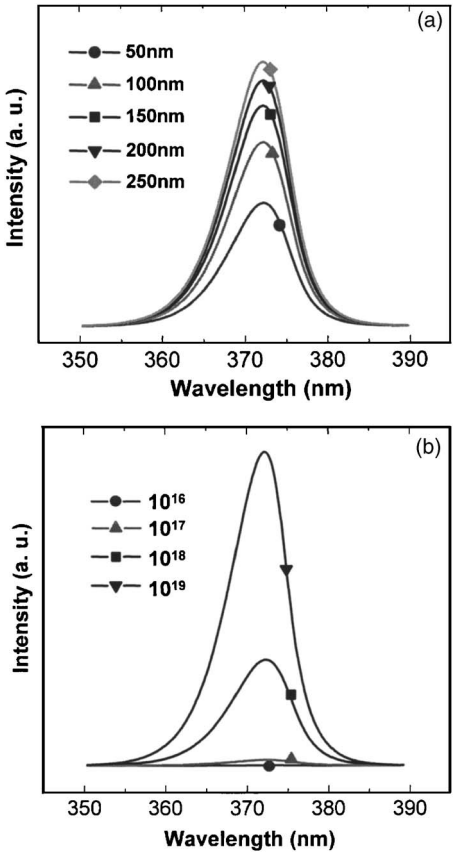


FIG. 4. Simulated emission spectra from ZnO/ZnCdO/ZnO/AlGaN/GaN structure as a function of either (a) active layer thickness and (b) doping concentration.

The simulated *I–V* characteristics did not show any significant dependence on either the thickness (in the range 50–250 nm) or Cd composition of the active layer (in the range 0.03–0.07). However, the doping level in the active region had a clear influence, as shown in Fig. 3. At very low doping levels ($\sim10^{16}$ $cm^{-3}$), the active region is depleted and the additional resistance pushes out the *I–V* characteristic.

Figure 4 shows the emission spectra as a function of the active layer thickness [Fig. 4(a)] and doping [Fig. 4(b)] for the ZnO/ZnCdO/ZnO/AlGaN/GaN structure. These results indicate that there is a significant increase in emission intensity for highly doped active regions, but only a small dependence on the active layer thickness above the limit for quantum wells. The simulated emission wavelength at ~370 nm is shorter than expected, due to the uncertainty concerning ZnCdO material parameters, including discontinuities and bowing parameter. The experimental band gap of our ZnCdO is ~2.9 eV and, therefore, we would expect the emission

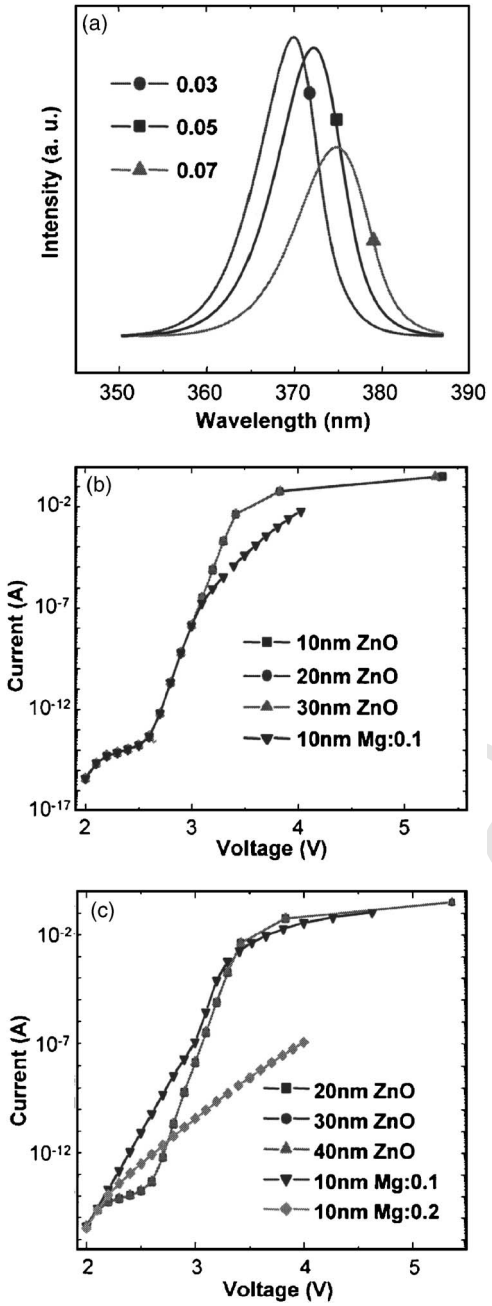


FIG. 5. (a) Simulated emission spectra from ZnO/ZnCdO/ZnO/AlGaN/GaN structure as a function of Cd composition. $I-V$ characteristics as a function of (b) top ZnO clad layer thickness and composition and (c) bottom ZnO clad layer thickness and composition.

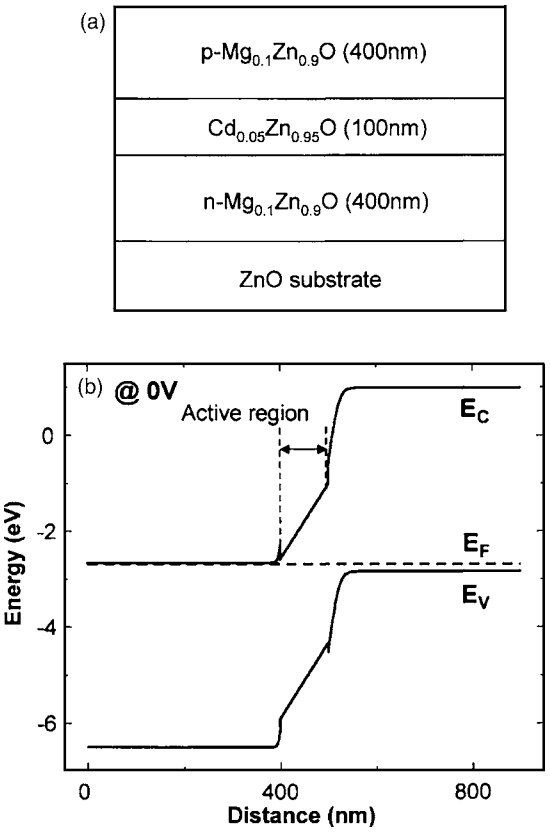


FIG. 6. (a) Schematic of MgZnO/ZnCdO/MgZnO structure simulated and (b) its band diagram.

wavelength to be ~2.9 eV or shorter due to triangular wells arising from the polarization contribution at the interfaces. However, in previous work on ZnCdO alloy films, the actual energy band gap of 5% Cd alloyed ZnCdO film was determined to be ~3.07 eV[18] and a reliable bowing parameter between ZnO and CdO is not available in the literature. In our simulations we used experimental data from Ref. 18, and assumed that the emission intensity is a function of material parameters.

Some additional parameters that had a significant effect on ZnO LED characteristics were obviously the Cd composition of the active layer [Fig. 5(a)] and the thickness and composition of the top and bottom cladding layers [Figs. 5(b) and 5(c)]. The light output is red-shifted as the Cd concentration increases, leading to a smaller bandgap of the ZnCdO. On the other hand, the $I-V$ characteristics were degraded by increasing the bandgap of the top and bottom cladding layers through Mg doping. These layers reduced the light output at fixed bias relative to the output when pure ZnO cladding layers were used. This implies that increasing the bandgap of the cladding layer is beneficial only when quantum wells are used to achieve better carrier confinement.

TABLE II. Simulated parameters conducted in MgZnO/ZnCdO/MgZnO structure. Bolded conditions in the table correspond to the referenced ones in Fig. 6.

| Parameters | Conditions |
|---|---|
| Active layer thickness | 30, 50, 75, **100**, 150, 200 (nm) |
| Active layer doping | **Undoped**, $10^{15}, 10^{16}, 10^{17}, 10^{18}, 10^{19}$ ($cm^{-3}$) |
| Active layer composition | Cd composition: 0.03, **0.05**, 0.07 |
| Cladding layer thickness | 300, **400**, 500 (nm) |
| Cladding layer doping | $10^{16}, 10^{17}, \mathbf{10^{18}}, 10^{19}$ ($cm^{-3}$) |
| Cladding layer composition | Mg composition: 0.05, **0.1**, 0.15, 0.2, 0.3 |

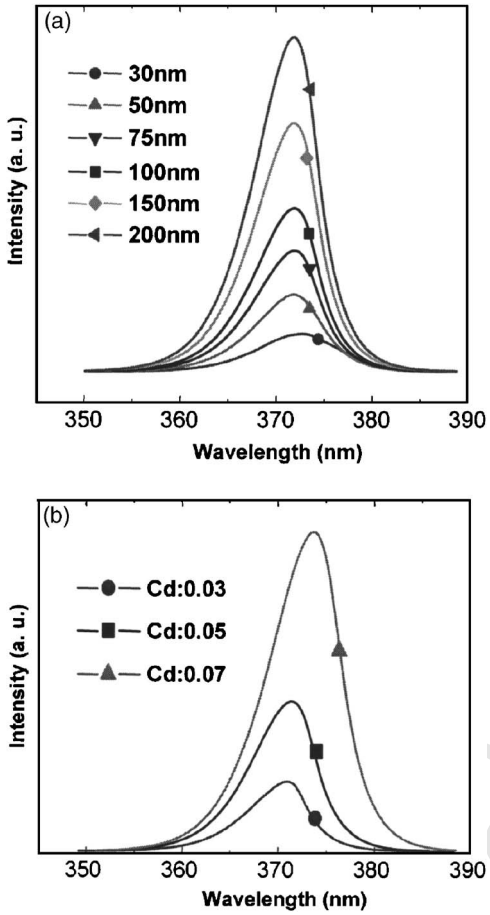


FIG. 7. Simulated emission spectra from MgZnO/ZnCdO/MgZnO structure as a function of both active layer (a) thickness and (b) Cd composition.

### B. ZnMgO/ZnCdO LEDs

Figure 6 shows a schematic of the MgZnO/ZnCdO/MgZnO structure on a ZnO substrate and a corresponding band diagram simulated with this structure. The bias condition in the band diagram was 0 V. The range of the various parameters for the simulations is summarized in Table II. The triangular wells arising from the polarization contribution at the interfaces were observed, but their magnitudes are much smaller than those for the hybrid ZnO/GaN structure. Our preliminary results have yielded only small band offsets in the ZnMgO/ZnO system (~0.14 eV in the conduction band and 0.02 eV in the valence band at ~5 at.% Mg).[23] Thus, we expect that the use of Cd to reduce the bandgap should increase these offsets.

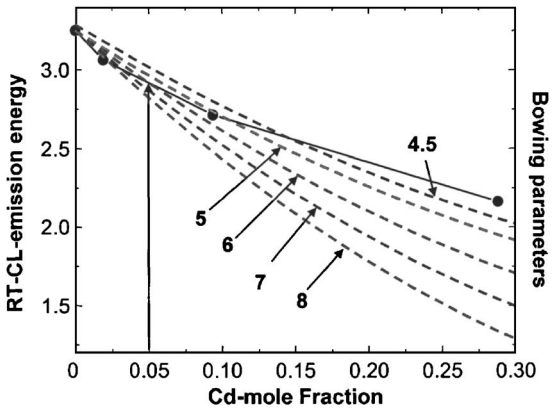


FIG. 8. Experimentally observed change of room-temperature cathodoluminescence emission energy (solid circles) and simulated bowing parameters (dashed lines) as a function of Cd mole fraction.

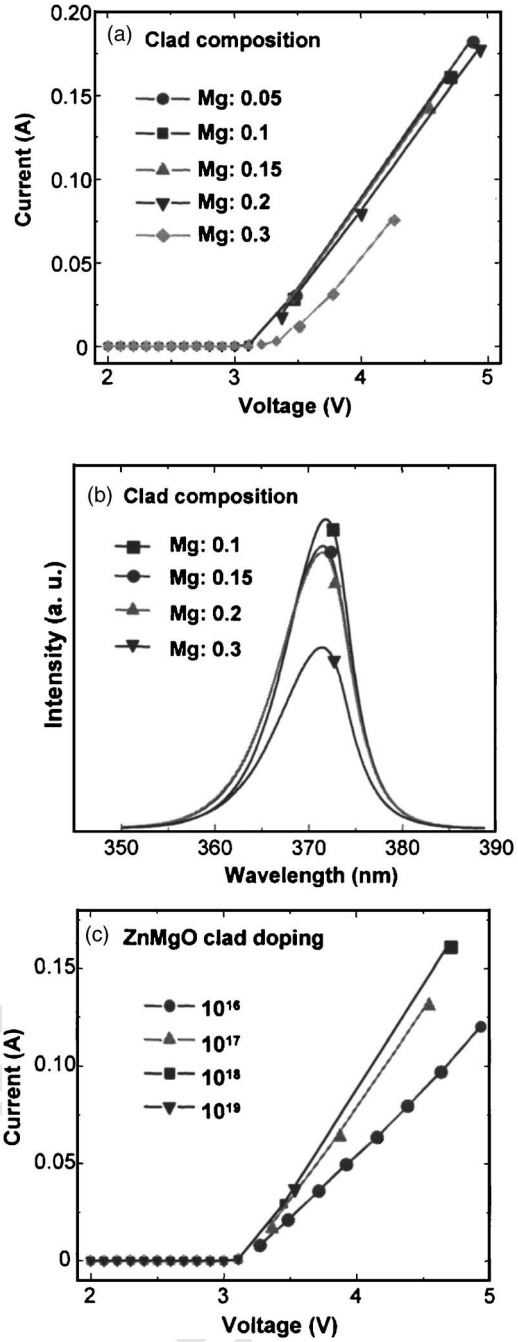


FIG. 9. Simulated (a) $I-V$ characteristics and (b) emission spectrum of MgZnO/ZnCdO/MgZnO structure as a function of clad layer composition. (c) $I-V$ characteristic as a function of clad layer doping.

The simulated emission spectra from MgZnO/ZnCdO/MgZnO as a function of active layer parameters are shown in Fig. 7. There is an increase in light output intensity with both

active layer thickness and Cd composition, as well as the expected red shift of the wavelength with increasing Cd content. Alternatively, the dependence of doping concentration on emission intensity was not significant when compared to that for thickness and doping. The series resistance of the active layer had no observable effect on the $I-V$ characteristics. This indicates that the LED optical properties are very sensitive to the physical parameters of the active region, so that optimization of the active layer design needs to focus on the emission properties rather than the electrical ones.

The simulated emission wavelength is obviously strongly dependent on the active layer composition and the choice of bowing parameters. Figure 8 shows both experimental data for the emission wavelength of CdZnO as a function of composition determined by Rutherford backscattering measurements and peak emission taken from the simulated spectral data for DHSs with different mole fraction of Cd as a function of Cd mole fraction. Since there is no phase separation in the CdZnO films, as confirmed by CL emission mapping, this fit is a practical calibration for adjustment of bowing parameters for CdZnO band gap dependence. In our case we use a bowing parameter of around 6 for a Cd composition of 5%.

As the ZnMgO cladding layer thickness was increased, the $I-V$ characteristics showed somewhat greater series resistance. On the other hand, the cladding layer thickness did not have much influence on the emission intensity. The most important effect of the cladding layers was the effect that the Mg composition had on the $I-V$ characteristics [Fig. 9(a)] because of the increased series resistance at high Mg content which also affected the emission intensity [Fig. 9(b)]. The doping of the cladding layer also affected the $I-V$ characteristics [Fig. 9(c)], but had only a minor impact on emission intensity.

## IV. SUMMARY AND CONCLUSIONS

Our work identified several key aspects of ZnO-based LEDs design. In the case of MgZnO/CdZnO heterojunctions grown on ZnO substrates, it is still necessary to obtain accurate measurements of the band offsets as a function of Mg and Cd composition. Active layer thickness and doping are important factors effecting emission intensity in these structures and the effect of polarization effects on *c*-plane substrates needs further study. The hybrid ZnO/GaN approach provides an alternative for achieving robust *p*-type doping for ZnO-based LED that incorporates ZnCdO active regions with optimized doping and thickness. Much more work needs to be done in determining basic materials parameters for both the ZnMgO and ZnCdO materials system so that a more accurate data base for simulations can be established.

## ACKNOWLEDGMENTS

The work at UF was supported in part by the Army Research Office under Grant No. DAAD19-01-1-0603, the Army Research Laboratory, the National Science Foundation (DMR 0400416, Dr. L. Hess), and the Air Force Office of Scientific Research under Grant No. F49620-03-1-0370. This work was also supported from the post-doctoral fellowship programs of Korea Science & Engineering Foundation (KOSEF) and Samsung Electro-Mechanics.

[1]D. C. Look, B. Claflin, Ya. I. Alivov, and S. J. Park, Phys. Status Solidi A **201**, 2203 (2004).
[2]D. C. Look, Mater. Sci. Eng., B **80**, 383 (2001).
[3]S. J. Pearton, D. P. Norton, K. Ip, Y. W. Heo, and T. Steiner, Prog. Mater. Sci. **50**, 293 (2005).
[4]Y. R. Ryu, T. S. Lee, J. H. Leem, and H. W. White, Appl. Phys. Lett. **83**, 4032 (2003).
[5]X.-L. Guo, J.-H. Choi, H. Tabata, and T. Kawai, Jpn. J. Appl. Phys., Part 2 **40**, L177 (2001).
[6]T. Aoki and Y. Hatanaka, Appl. Phys. Lett. **76**, 3257 (2000).
[7]Y. I. Alivov, J. E. Van Nostrand, D. C. Look, M. V. Chukichev, and B. M. Ataev, Appl. Phys. Lett. **83**, 2943 (2003).
[8]Y. I. Alivov, E. V. Kalinina, A. E. Cherenkov, D. C. Look, B. M. Ataev, A. K. Omaev, M. V. Chukichev, and D. M. Bagnall, Appl. Phys. Lett. **83**, 4719 (2003).
[9]H. Hosono, H. Ohta, K. Hayashi, M. Orita, and M. Hirano, J. Cryst. Growth **237–239**, 496 (2001).
[10]A. Osinsky, J. W. Dong, M. Z. Kauser, B. Hertog, A. M. Dabiran, P. P. Chow, S. J. Pearton, O. Lopatiuk, and L. Chernyak, Appl. Phys. Lett. **85**, 4272 (2004).
[11]J. W. Dong, A. Osinsky, B. Hertog, A. M. Dabiran, P. P. Chow, Y. W. Heo, D. P. Norton, and S. J. Pearton, J. Electron. Mater. **34**, 416 (2005).
[12]Dae-Kue Hwang, Soon-Hyung Kang, Jae-Hong Lim, Eun-Jeong Yang, Jin-Yong Oh, Jin-Ho Yang, and Seong-Ju Park, Appl. Phys. Lett. **86**, 222101 (2005).
[13]A. Tsukazaki, A. Ohtomo, T. Onuma, M. Ohtani, T. Makino, M. Sumiya, K. Ohtani, S. F. Chichibu, S. Fuke, Y. Segawa, H. Ohno, H. Koinuma, and M. Kawasaki, Nat. Mater. **4**, 42 (2005).
[14]A. Tsukazaki, M. Kubota, A. Ohtomo, T. Onuma, K. Ohtani, H. Ohno, S. F. Chichibu, and M. Kawasaki, Jpn. J. Appl. Phys., Part 2 **44**, L643 (2005).
[15]A. Ohtomo, M. Kawasaki, I. Ohkubo, H. Ko inuma, T. Yasuda, and Y. Segawa, Appl. Phys. Lett. **75**, 980 (1999).
[16]F. P. Koffyberg, Phys. Rev. B **13**, 4470 (1976).
[17]See, for example, http://www.semitech.us/products/SiLENSe/
[18]T. Makino, Y. Segawa, M. Kawasaki, A. Ohtomo, R. Shiroki, K. Tamura, T. Yasuda, and H. Koinuma, Appl. Phys. Lett. **78**, 1237 (2001).
[19]D. P. Norton, Y. W. Heo, M. P. Ivill, K. Jp, S. J. Pearton, M. F. Chisholm, and T. Steiner, Mater. Today **7**, 34 (2004).
[20]http://www.semiconductors.co.uk.
[21]http://www.onr.navy.mil/sci_tech/information/312_electronics/ncsr.
[22]A. Osinsky, J. W. Dong, M. Z. Kauser, B. Hertog, A. M. Dabiran, C. Plaut, P. P. Chow, S. J. Pearton, X. Y. Dong, and C. J. Palmstrom, Electrochem. Soc. **2004–06**, 211 (2004).
[23]A. Osinsky, J. W. Dong, J. Q. Xie, B. Hertog, A. M. Dabiran, P. P. Chow, S. J. Pearton, D. C. Look, W. Schoenfeld, O. Lopatiuk, and L. Chemyak, MRS Fall Meeting, Boston, Nov. 2004.